Transactions of the Korean Nuclear Society Spring Meeting
Jeju, Korea, May 9-10, 2024

Deep Learning-based Beam Profile Restoration for Real-time Proton Beam Monitoring

Gwang-il Jung[a,b*], Young Seok Hwang [a], Chan Young Lee [a], Jun Mok Ha [a], Yu Mi Kim [a], Eun Joo Oh [a], Jimin Lee[b,*]
[a]*Beam Utilization Research Division, Korea Atomic Energy Research Institute, 181 Miraero, Gyeoncheon-eup, Gyeongju 38180*
[b]*Department of Nuclear Engineering, Ulsan National Institute of Science and Technology, 50 UNIST-gil, Eonyang-eup, Ulju-gun, Ulsan 44919*
[*]*Corresponding author: jiminlee@unist.ac.kr*

***Keywords :** deep learning, beam profile, U-Net, image restoration

1. Introduction

The Korea-Multi-Purpose Accelerator Complex (KOMAC) operates a 100 MeV proton linear accelerator, providing a high flux proton beam at the TR103, a general-purpose irradiation facility. A real-time and in-situ proton beam profiles monitoring system which includes a P43 (ProxiVision) phosphor screen and CMOS camera was recently introduced and tested at the TR103. However, since this system is installed in air, various factors degrade the quality of the beam profile images including high level background, hot pixels caused by secondary radiation exposure [1], and saturation of the beam profile under the high flux proton irradiation. In this study, we employed U-Net, a deep learning model, to effectively restore noisy and saturated beam profiles to approximate their true beam profiles [2].

2. Methods and Results

This section describes several methods to generate datasets for deep learning training. To prepare a large dataset, virtual beam profiles with background noise and virtual saturated beam profiles were generated using Python [3].

2.1 Virtual Beam Profile Datasets

The beam profile datasets needed to train a deep learning model that restores the noisy beam profile to the true beam profile were virtually generated. For generating ground truth beam profiles, in an image size of 400×400 pixel, the location, sigma in the x and y directions of the beam profile were randomly selected. For generating noisy beam profiles to be used as input for model training, one of the five kinds of real background image was randomly selected and multiplied to the ground truth beam profile as shown in Fig. 1. When the flux level of a proton beam exceeds a certain threshold, the camera reaches its limit of acceptable light, resulting in the truncation of the upper portion of the beam profile. Therefore, to replicate this phenomenon with a virtual beam profile, the saturated region was modeled using a super gaussian function as shown in Fig. 2. The sigma values of the inner super gaussian function and outer gaussian function, along with the location of their boundaries and the beam profile, were randomly selected. Datasets comprising 3,500 input-target pairs were prepared for both the noisy beam profile and the saturated beam profile.

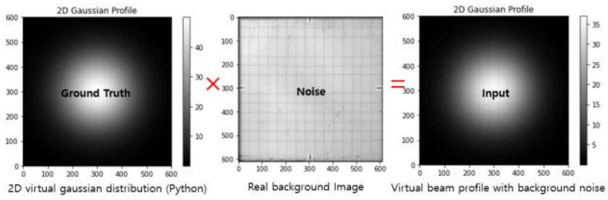

Fig. 1. Process of generating a dataset of virtual beam profile with background noise

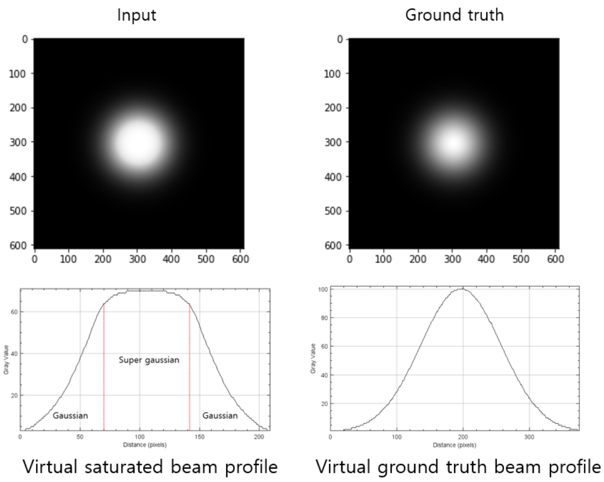

Fig. 2. Process of generating a dataset of virtual saturated beam profile.

2.2 Deep Learning Model

The U-Net architecture comprises a contracting path for context extraction and an expanding path for precise localization as shown in Fig. 3. The contracting path includes convolutional layers followed by max-pooling for down-sampling, while the expanding path involves up-sampling followed by convolutional layers for feature refinement. Skip connections between corresponding layers maintain spatial information, facilitating accurate reconstruction of the true beam profile from both noisy and saturated beam profile inputs. To find the optimal model for efficient beam profile recovery, we trained six kinds of the U-Net architecture by adjusting the number of layers, nodes, and up-sampling methods. U-Net #1, #2, and #3 are categorized based on the number of layers and nodes. U-Net 1 has the following structure: [(1,64), (64,128), (128,256), (256,512), (512,1024)]. U-Net #2 has a structure of: [(1,64), (64,128), (128,256), (256,512)]. Lastly, U-Net 3 has a structure of: [(1,32), (32,64), (64,128), (128,256)]. Adam optimizer [4] was used, employing Mean Squared Error (MSE) loss for restoring the noisy beam profile and MS-SSIM loss for the saturated beam profile restoration [5]. The dataset was split into training, validation, and test sets, consisting of 3000, 400, and 100 samples, respectively.

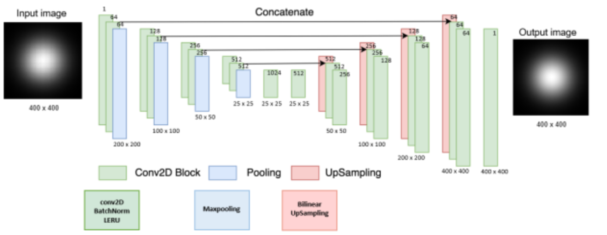

Fig. 3. The architecture of U-Net #1 for restoration of noisy and saturated beam profile.

2.3 Model Selection

To evaluate the six trained models aimed at restoring the noisy beam profile and saturated beam profile, the average Peak Signal-to-Noise Ratio (PSNR) and Structural Similarity Index (SSIM) values between the output image from the models and the target image for 100 test data samples were computed. These results are summarized in Table 1 and Table 2, respectively. (In tables, "bc" and "bl" denotes bicubic and bilinear interpolation of up-sampling methods.) As shown in Table 1, for the restoration of the noisy beam profile, the U-Net #2-bl architecture with [(1,64), (64,128), (128,256), (256,512)] and bilinear up-sampling exhibited the highest PSNR and SSIM values among all models. Conversely, for the restoration of the saturated beam profile, the U-Net #1-bc architecture with [(1,64), (64,128), (128,256), (256,512), (512,1024)] and bicubic up-sampling exhibited the highest PSNR and SSIM values as shown in Table 2.

Table 1: Average PSNR and SSIM Results for Six Models in Noisy Beam Profile Restoration

	U-Net #1-bl	U-Net #1-bc	**U-Net #2-bl**	U-Net #2-bc	U-Net #3-bl	U-Net #3-bc
PSNR	36.72	42.57	**46.95**	46.61	46.71	46.69
SSIM	0.9192	0.9897	**0.9913**	0.9891	0.9889	0.989

Table 2: Average PSNR and SSIM Results for Six Models in Saturated Beam Profile Restoration

	U-Net #1-bl	**U-Net #1-bc**	U-Net #2-bl	U-Net #2-bc	U-Net #3-bl	U-Net #3-bc
PSNR	36.79	**41.62**	40.34	19.53	23.59	38.19
SSIM	0.9879	**0.9925**	0.9929	0.9508	0.9781	0.9944

2.5 Beam Profile Restoration

Utilizing the selected models, the saturated and noisy beam profile measured using the phosphor screen were restored to the true beam profile. Firstly, the 20 MeV proton beam profile was captured using a phosphor screen and a CMOS camera, and then cropped to a size of 400×400 pixel. Secondly, the cropped image was fed into the input of the U-Net #2-bl model to obtain the denoised beam profile image. Thirdly, the denoised image was fed into the input of the U-Net #1-bc model to obtain the desaturated beam profile image. Fig 4. illustrates the process of reconstructing the true beam profile from the noisy and saturated beam profile, along with its comparison to the measurement obtained from the HD-V2 film (Gafchromic^{TM}).

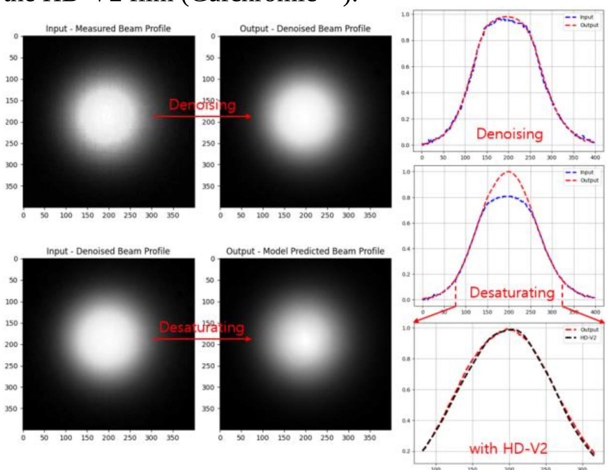

Fig. 4. The process of reconstructing the true beam profile from the noisy and saturated beam profile and its comparison to the measured beam profile obtained from the HD-V2 film.

3. Conclusions

U-Net, a deep learning model, was employed to restore noisy and saturated beam profile to the true beam profiles. To prepare datasets for training deep learning models, virtual beam profiles with background noise and virtual saturated beam profiles were generated using Python. To find the optimal model for efficient beam profile restoration, six kinds of the U-Net architecture by adjusting the number of layers, nodes, and up-sampling methods were trained. The U-Net #2-bl model was selected for restoring the noisy beam profile, while the U-Net #1-bc model was selected for restoring the saturated beam profile. It was successfully verified that the selected models closely approximated the measurement obtained from the HD-V2 film in restoring the beam profile. These models will enable precise real-time monitoring of beam profiles by effectively restoring noisy and saturated proton beam profiles.

REFERENCES

[1] A. Huber, G. Sergienko, D. Kinna, and V. Huber, Response of the imaging cameras to hard radiation during JET operation, Fusion Engineering and Design, vol. 123, pp.669-673, 2017.

[2] O. Ronneberger, P. Fischer, T. Brox, U-Net: Convolutional Networks for Biomedical Image Segmentation, In Medical Image Computing and Computer-Assisted Intervention, vol. 9351, pp. 234-241, 2015.

[3] Python Software Foundation License Version 2.

[4] Diederik P. Kingma and Jimmy Ba, Adam: A Method for Stochastic Optimization, arXiv preprint arXiv:1412.6908, 2014.

[5] Z. Wang, E. P. Simoncellie and A. C. Bovik, Multiscale Structural Similarity for Image Quality Assessment, The Thirty-Seventh Asilomar Conference on Signals, Systems & Computers, vol. 2, pp. 1398-1402, 2003.